Adaptive Sensitivity Encoding Incorporating Temporal Filtering (TSENSE)

Peter Kellman,* Frederick H. Epstein, and Elliot R. McVeigh

A number of different methods have been demonstrated which increase the speed of MR acquisition by decreasing the number of sequential phase encodes. The UNFOLD technique is based on time interleaving of *k*-space lines in sequential images and exploits the property that the outer portion of the field-of-view is relatively static. The differences in spatial sensitivity of multiple receiver coils may be exploited using SENSE or SMASH techniques to eliminate the aliased component that results from undersampling *k*-space. In this article, an adaptive method of sensitivity encoding is presented which incorporates both spatial and temporal filtering. Temporal filtering and spatial encoding may be combined by acquiring phase encodes in an interleaved manner. In this way the aliased components are alternating phase. The SENSE formulation is not altered by the phase of the alias artifact; however, for imperfect estimates of coil sensitivities the residual artifact will have alternating phase using this approach. This is the essence of combining temporal filtering (UNFOLD) with spatial sensitivity encoding (SENSE). Any residual artifact will be temporally frequency-shifted to the band edge and thus may be further suppressed by temporal low-pass filtering. By combining both temporal and spatial filtering a high degree of alias artifact rejection may be achieved with less stringent requirements on accuracy of coil sensitivity estimates and temporal low-pass filter selectivity than would be required using each method individually. Experimental results that demonstrate the adaptive spatiotemporal filtering method (adaptive TSENSE) with acceleration factor $R = 2$, for real-time nonbreath-held cardiac MR imaging during exercise induced stress are presented. Magn Reson Med 45:846–852, 2001. Published 2001 Wiley-Liss, Inc.†

Key words: SENSE; SMASH; UNFOLD; rapid imaging; cardiac imaging; parallel MRI

A number of different methods (1–3) have been demonstrated which increase the speed of MR acquisition by decreasing the number of sequential phase encodes. The UNFOLD technique (1) is based on time interleaving of *k*-space lines in sequential images and exploits the property that the outer portion of the field-of-view (FOV) is relatively static. The SENSE (2) and SMASH (3) techniques exploit the differences in spatial sensitivity of multiple receiver coils to eliminate the aliased component that results from undersampling *k*-space. In this article, we present an adaptive method of sensitivity encoding which incorporates both spatial and temporal filtering.

Temporal filtering is incorporated with spatial encoding by acquiring phase encodes in an interleaved manner, as in UNFOLD (i.e., alternating between even and odd lines). In this way the aliased components are alternating phase, thus the alias artifact is temporally frequency-shifted to the band edge and may be suppressed by temporal low-pass filtering. The phase of the alias artifact does not alter the SENSE formulation (inverse solution). However, if the estimates of coil sensitivities are imperfect, there will be residual alias artifacts. This is the essence of combining temporal filtering (UNFOLD) with spatial sensitivity encoding (SENSE). Any residual artifact will be temporally frequency-shifted to the band edge and thus may be further suppressed by temporal low-pass filtering.

By combining both temporal and spatial filtering the resulting implementation achieves a high degree of alias artifact rejection with less stringent requirements on accuracy of coil sensitivity estimates and temporal low-pass filter selectivity than would be required using each method individually. Spatial nulling of alias artifacts is accompanied by noise amplification that results in a loss in signal-to-noise ratio (SNR). Since the degree of spatial nulling or artifact suppression may be relaxed using the combined method, this permits a more flexible design tradeoff between null depth and SNR loss. This may be accomplished by regularizing the inverse solution to reduce the ill-conditioning (4).

This method is adaptive since the coil sensitivities are derived from the data itself and, therefore, do not require a separate image acquisition. Benefits of the adaptive algorithm are the ability to track changes in relative coil sensitivities over time, which may arise due to chest wall or other body motion, as well as the time savings by elimination of a separate reference acquisition. Adaption may be useful when continuous, interactive scan plan motion is desired, such as in interventional MR application.

We present experimental results that demonstrate the adaptive spatiotemporal filtering method (TSENSE) for real-time nonbreath-held cardiac imaging. An acceleration factor of $R = 2$ is used in this example. In nonbreath-held applications such as exercise stress testing or interventional MRI, the assumption made by UNFOLD that the outer portion of the FOV is relatively static is not always met, particularly due to chest wall motion. Similarly, the assumption made by SENSE that the coil sensitivities are static is also not perfectly met. As a result, alias artifacts are not completely removed. The combined method is shown to achieve additional artifact suppression. An additional benefit of this approach is that artifact suppression may be measured quantitatively by analysis of the temporal spectrum of individual pixels.

This method may be implemented with a variable density *k*-space sampling scheme (i.e., increased sampling of central *k*-space) to further increase artifact suppression (5). The use of combined temporal and spatial filtering may be

Laboratory of Cardiac Energetics, National Institutes of Health, National Heart, Lung and Blood Institute, Bethesda, Maryland.

*Correspondence to: Peter Kellman, Laboratory of Cardiac Energetics, National Institutes of Health, National Heart, Lung and Blood Institute, 10 Center Drive, MSC-1061, Building 10, Room B1D416, Bethesda, MD 20892-1061. E-mail: kellman@nih.gov

employed with either SMASH or SENSE methods. Previous work combining UNFOLD with SENSE or SMASH was aimed at increased acceleration (6). Extension of TSENSE to higher acceleration factors may be performed with *N*-fold interleaving in a variety of schemes. The aim of this work is an algorithm that achieves a high degree of alias artifact suppression with reduced sensitivity to motion and other errors.

METHODS

Theory

The UNFOLD technique (1) is based on acquiring *k*-space phase encode lines in a time-interleaved fashion, i.e., the sequence acquisition alternates between even and odd lines to increase the frame rate by a factor of $R = 2$. The images reconstructed from either the even or odd lines have aliasing, which results from halving the FOV. The sign of the aliased component is alternating, thus the aliased component is shifted in temporal frequency and may be rejected by means of low-pass temporal filtering.

The SENSE (2) technique exploits the differences in spatial sensitivity of multiple receiver coils to eliminate the aliased component that results from undersampling *k*-space. The formulation of $R = 2$ sensitivity encoding (SENSE) may be readily extended to time-interleaved *k*-space acquisition by expressing the reconstructed coil images in matrix form and including the alternating sign of the aliased component:

$$\begin{bmatrix} \tilde{f}_1(x, y, t) \\ \vdots \\ \tilde{f}_N(x, y, t) \end{bmatrix} = \begin{bmatrix} s_1(x, y) & s_1(x, y \pm FOV/2) \\ \vdots & \vdots \\ s_N(x, y) & s_N(x, y \pm FOV/2) \end{bmatrix}$$
$$\times \begin{bmatrix} f(x, y, t) \\ f(x, y \pm FOV/2, t)(-1)^t \end{bmatrix}, \quad [1]$$

where *f(x, y, t)* represents the desired sequence of images, $\tilde{f}_i(x, y, t)$ is the reconstructed sequence of images for the *i*-th coil, $s_i(x,y)$ is the complex sensitivity profile for the *i*-th coil, *N* denotes the number of coils, and the alternating sign factor $(-1)^t$ is due to the interleaved *k*-space acquisition. The desired unaliased full FOV images *f(x,y,t)* may be computed from the measured aliased images $\tilde{f}_i(x,y,t)$, assuming the coil sensitivities are known or estimated with sufficient accuracy. The generalized weighted least-squares solution (2) is given by:

$$\hat{\mathbf{f}}_{\mathbf{SENSE}} = (\hat{\mathbf{S}}^H \mathbf{R_n^{-1}} \hat{\mathbf{S}})^{-1} \hat{\mathbf{S}}^H \mathbf{R_n^{-1}} \tilde{\mathbf{f}} = \mathbf{U}\tilde{\mathbf{f}}, \quad [2]$$

where $\tilde{\mathbf{f}}$ denotes the *N*x1 vector of aliased images (for each coil), $\hat{\mathbf{f}}_{\mathbf{SENSE}}$ denotes the 2x1 vector estimate of unaliased images, $\hat{\mathbf{S}}$ is the estimated sensitivity matrix, $\mathbf{R_n}$ is the estimated noise correlation matrix between coils, and $\mathbf{U}$ is defined as the unmixing matrix.

The phase of the alias artifact (± 1 in this case) which results from the interleaved *k*-space acquisition order does not alter the SENSE formulation (inverse solution of Eq. [2]). However, if the estimates of coil sensitivities are imperfect there will be residual artifacts. Any residual artifact will be temporally frequency-shifted to the band edge
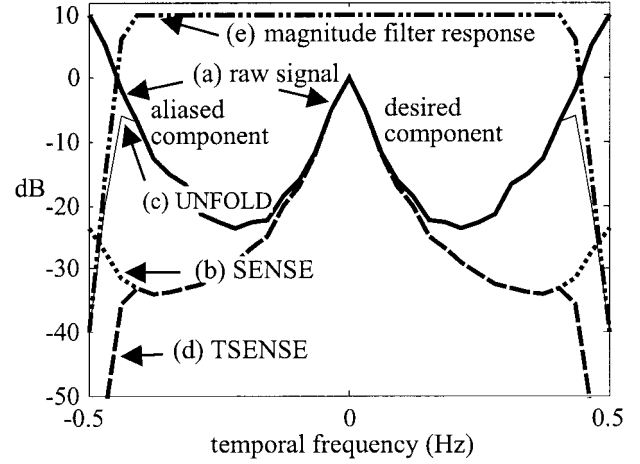
FIG. 1. Illustration of temporal spectrum of a pixel with (**a**) raw signal showing both desired and aliased components, (**b**) SENSE, (**c**) UNFOLD, and (**d**) TSENSE, with (**e**) low-pass filter response overlaid.

and thus may be further suppressed by temporal low-pass filtering. It may be readily observed due to the linearity of both UNFOLD and SENSE that the spatial and temporal filtering operations may be performed in either order. Thus the TSENSE estimate is defined as:

$$\hat{f}_{TSENSE}(x, y, t) = [\hat{\mathbf{f}}_{\mathbf{SENSE}}(x, y, t)]_{(1,1)} * h_{LPF}(t)$$
$$= [\mathbf{U}\hat{\mathbf{f}}_{\mathbf{UNFOLD}}]_{(1,1)}, \quad [3]$$

where $\hat{f}_{UNFOLD,i}(x,y,t) = \tilde{f}_i(x,y,t) * h_{LPF}(t)$ is the temporally filtered image for the *i*-th coil, $h_{LPF}(t)$ denotes the temporal low-pass filter impulse response, and the asterisk ($*$) denotes the convolution operation. While either order may be mathematically equivalent, it is computationally advantageous to temporally filter after combining the multiple coils (i.e., perform SENSE followed by UNFOLD).

The principle of UNFOLD is to separate the desired component, *f(x,y,t)*, from the undesired aliased component, $f(x,y\pm FOV/2)(-1)^t$ by means of low-pass temporal filtering. Each pixel in the aliased image is a mixture of two components that share the same bandwidth. More bandwidth can be allocated to the desired image component if the aliased image region is relatively static with correspondingly less temporal bandwidth.

Figure 1 illustrates the temporal spectrum of a pixel with both desired and aliased components. The two-sided spectra is shown to represent the fact that, in general, the signal is complex and will have an asymmetric spectrum resulting from phase modulation. In this example, chosen to illustrate the benefit of the TSENSE method, it is assumed that the aliased region has significant motion and, therefore, the aliased component has a significant bandwidth which overlaps the spectrum of the desired component. This violates the typical assumption that when using UNFOLD the peripheral FOV should be relatively static. The use of the UNFOLD method by itself would be unable to completely suppress the artifact if it is to provide the increase in bandwidth commensurate with the accelerated

imaging speed. However temporal low-pass filtering (UN-FOLD) does provide a high degree of suppression at the band edge where the aliased component is the strongest. The SENSE method provides suppression of the aliased component which is more uniform across the temporal spectrum (assuming static coil sensitivities).

While the central portion of FOV is typically more dynamic with correspondingly greater temporal bandwidth, the alias artifact due to the central FOV is weaker since it is further from the surface coils. Therefore, even in the peripheral FOV, spatial filtering should be able to provide the required suppression within the temporal passband. The TSENSE method still benefits from temporal low-pass suppression of the stronger average alias component at the band edge. Therefore, the low-pass filter may have a fixed (wide) bandwidth over the full FOV, in contrast with the normal UNFOLD bandwidth sharing assumption. In this case, temporal filtering may be performed in either the image or *k*-space domains (equivalent to some Fourier interpolation schemes).

The loss in SNR for reduced *k*-space acquisition relative to the full *k*-space acquisition is proportional to the square root of the acceleration factor, *R*. The expression for SNR is given as:

$$SNR_{TSENSE} = \frac{1}{G_{SENSE}} \sqrt{\frac{BW_{FULL}}{BW_{UNFOLD}}} \sqrt{\frac{1}{R}} \, SNR_{FULL} \, , \quad [4]$$

where BW_{FULL} which equals the sample rate and $BW_{UNFOLD} = \int |H(f)|^2 \, df/|H(0)|^2$ for low-pass filter $H(f)$ are the two-sided noise equivalent temporal bandwidths for full and reduced FOV *k*-space acquisitions, respectively, and G_{SENSE} is the noise amplification factor (2) which results from the inverse solution. The slight loss in temporal bandwidth due to the UNFOLD low-pass filter results in a slight SNR gain (BW_{UNFOLD}/BW_{FULL} is typically 0.8). The SNR loss ($1/G_{SENSE}$) due to the ill-conditioning of the coil sensitivity matrix depends on the *x,y* position, the specific array geometry, and the acceleration factor.

Adaptive Sensitivity Estimates

In the derivation above (Eq. [1]), the complex field sensitivities $s_i(x,y)$ for each coil were assumed to be static and known. An adaptive method for estimating the coil sensitivities is presented which may be readily incorporated with the TSENSE approach. The benefit of an adaptive estimate is the ability to track change that may result from breathing or other relative motion of the receive coils. The basis of the adaptive approach is to estimate the sensitivities from the raw data acquired with sequential interleaving of *k*-space (reduced FOV) by temporal filtering to suppress the alias artifact.

In order to estimate the field sensitivities $s_i(x,y)$, it is necessary to acquire full FOV unaliased images. This is normally accomplished by a separate acquisition of the full *k*-space data. Furthermore, it is customary to acquire the reference data using both the multicoil array as well as a body coil with uniform field sensitivity, in order to remove the dependence of the estimates on the image. In the adaptive TSENSE method, the unaliased images are
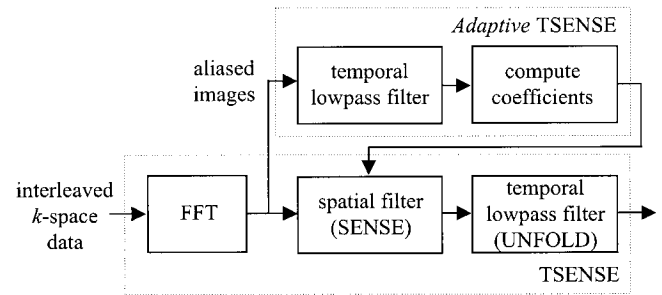
FIG. 2. Simplified block diagram for TSENSE and adaptive TSENSE.

reconstructed directly from the reduced FOV aliased images by means of temporal low-pass filtering similar to the UNFOLD method. The adaptive version of the TSENSE method is diagrammed in Fig. 2. Unlike the UNFOLD temporal filter, the bandwidth of the low-pass filter used for computing the spatial filter coefficients (upper portion of diagram) is designed to eliminate the aliased components almost completely. This causes temporal smearing of the reference image but still permits estimation of the relative coil sensitivities. Filtering also results in increased SNR for the raw coil sensitivity estimates. Further spatial smoothing may be desirable as well. The temporal bandwidth used for the coil sensitivity estimates may be made wide enough to track relatively slow variations, such as those from breathing or scan plane manipulation.

In this diagram SENSE precedes the UNFOLD (bottom portion of the diagram) to reduce the computation. Care must be taken to compensate for (not shown in simplified diagram), or minimize, any differential delay between the estimation and application of spatial filter coefficients (top and bottom portions of diagram) which might arise due to latency in the low-pass estimation filter.

In the adaptive method, without separate acquisition of reference data, the estimates are normalized by the root sum of squared magnitudes since the uniform field body coil data is not available on a continuous basis. By normalizing in this manner the image phase is not removed. In practice it is necessary to perform some degree of either spatial and/or temporal smoothing to the normalized raw coil images in order to achieve reasonable alias artifact suppression. In order to apply spatial smoothing to the complex coil data, the rapidly varying image-dependent phase must first be removed.

The TSENSE method may be used in conjunction with partial-NEX acquisition for increased speed. In this case, partial Fourier (homodyne) reconstruction is done at the final stage after temporal low-pass filtering. In the adaptive TSENSE implementation, the coil sensitivities are estimated from the full Fourier lower resolution images reconstructed with a spatial bandwidth corresponding to the amount of overscan. This is done to minimize homodyne artifacts in the coil sensitivity estimates. This detail is omitted from the simplified diagram shown in Fig. 2.

Variable Density *k*-Space Acquisition

The central *k*-space lines may be sampled at the full rate (i.e., $\Delta k = 1/FOV$) with minimal loss in overall accelerated

acquisition speed. The main advantage of increased sampling of the central *k*-space lines is the further suppression in alias artifacts (5). This can be seen by rewriting Eq. [1] to incorporate full FOV sampling of the central phase encodes:

$$
\begin{bmatrix} \tilde{f}_1(x, y, t) \\ \vdots \\ \tilde{f}_N(x, y, t) \end{bmatrix} = \begin{bmatrix} s_1(x, y) & s_1(x, y \pm FOV/2) \\ \vdots & \vdots \\ s_N(x, y) & s_N(x, y \pm FOV/2) \end{bmatrix}
$$
$$
\times \begin{bmatrix} f(x, y, t) \\ f(x, y \pm FOV/2, t) * h_{HPF}(y)(-1)^t \end{bmatrix}, \quad [5]
$$

where convolution with $h_{HPF}(y)$ corresponds to high-pass spatial filtering of frequencies which are fully sampled in *k*-space. The resulting aliased artifact has been high-pass spatial filtered which serves to reduce both the average and peak level of aliased artifact.

Experimental Parameters

Imaging of the heart was conducted following exercise-induced stress. A modified MR compatible ergometer (Lode, Groningen, The Netherlands) was used in a supine position. Image acquisition began approximately 15 sec after exercise while breathing was still very heavy. Heart rates were approximately 150 bpm and respiratory rates were approximately 30 breaths per minute. All individuals in this study were normal, healthy volunteers. This study was approved by the Institutional Review Board of the National Heart, Lung, and Blood Institute.

Imaging was performed using a GE Signa CV 1.5T MR Imager. A real-time fast gradient recalled echo train (FGRE-ET) pulse sequence (7) was used. Imaging was performed with sequential interleaving of odd and even phase encode lines. Data was reconstructed offline using the adaptive TSENSE algorithm. A four-element cardiac phased array coil was used.

Cardiac imaging of a short axis slice was performed at 31.2 frames per second using the following parameters. An echo train length (*ETL*) of eight echoes was used with ± 125 kHz bandwidth and a repetition interval $T_R = 10.7$ msec. The flip angle was 15°, with a slice thickness of 10 mm. The FOV was 380×190 mm (1/2 FOV) with an image matrix of 128 frequency encodes $\times$ 96 phase encodes; thus, the in-plane spatial resolution was approximately 3×4 mm. Better spatial resolution may be achieved by use of partial-NEX acquisition of fewer phase encodes or by making other tradeoffs. The number of *k*-space lines acquired for 1/2 FOV was 48. The 48 phase encodes were acquired in an interleaved manner, 24 odd lines followed by 24 even, and so forth. Thus each of the 24 phase encodes were acquired in 3 T_R's resulting in a frame period of $3 \times 10.7 = 32.1$ msec (approximately 31.2 frames/sec). The real-time sequence was continuous (i.e., not triggered). Several seconds of data (between 2 and 10) were acquired for off-line analysis. Echo-shifting was employed to reduce EPI ghosting artifacts.

The magnitude frequency response specifications of the UNFOLD temporal low-pass filter were: $f_p = 0.4$ (passband cutoff), corresponding to 80% of the available bandwidth, $R_p = 1.5$ dB (passband flatness), $f_s = 0.49$ (stopband fre-
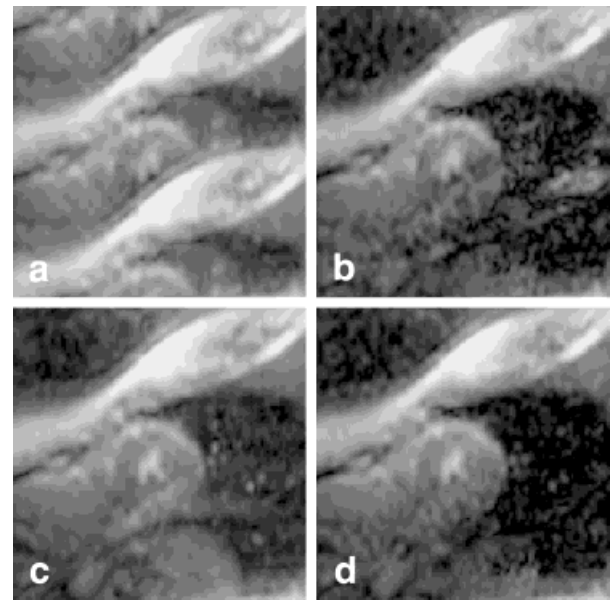
FIG. 3. Example real-time cardiac short axis images near end-systole for exercise induced stress at a heart rate of 150 bpm showing (**a**) raw aliased image, (**b**) image after spatial filter (SENSE), (**c**) image after temporal filter (UNFOLD), (**d**) image after combined adaptive spatiotemporal filter (TSENSE).

quency), $R_s = 50$ dB (stopband rejection), with all frequencies normalized by the sample rate. The low-pass filter used for the adaptive estimates of complex coil sensitivity profiles had a low-pass bandwidth of 0.75 Hz. Similar results were obtained using adaption bandwidths up to 2.5 Hz. No spatial smoothing or thresholding were used in either case.

The SNR loss for TSENSE relative to the full *k*-space reconstruction (Eq. [4]) was measured by imaging a cylindrical water phantom (approximately 20 cm diameter) with the four-element cardiac coil (axial images). Sensitivity profiles for each coil were calculated using temporal averaging of 32 frames and applying 3×3 spatial smoothing. The UNFOLD temporal filter specified above was used for the phantom SNR measurements. A total of 256 consecutive images were acquired and the SNR was estimated for each pixel using the 256 point sample mean and variance. SNR measurements for UNFOLD, SENSE, and TSENSE reconstructions were then compared with SNR estimates for full *k*-space reconstruction.

RESULTS AND DISCUSSION

Example single slice, short axis images of the heart reconstructed with different methods are shown in Figs. 3 and 4 for cardiac phases near end-systole and mid-diastole, respectively. These images were chosen to illustrate conditions where both UNFOLD and SENSE had difficulty achieving complete artifact suppression, as will be described below. Figures 3a and 4a illustrate the raw aliased reconstruction. In this example, the chest wall aliases directly on the posterior lateral portion of the heart. Furthermore, the chest wall intensity is several times that of the myocardium of interest due to the proximity of the surface
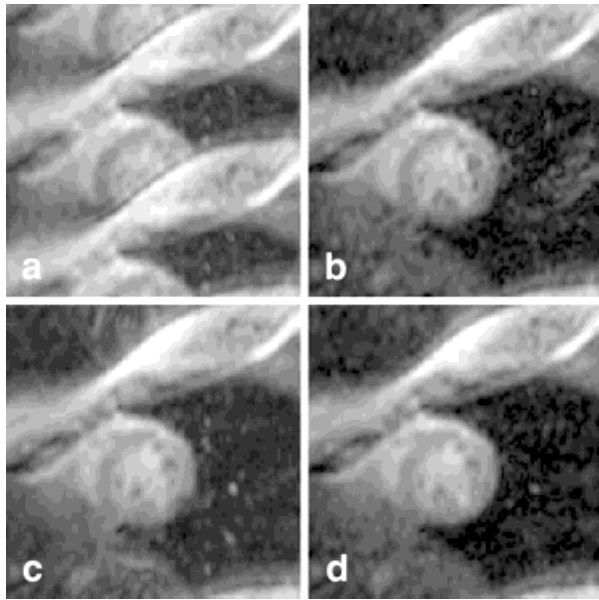
FIG. 4. Example real-time cardiac short axis images near mid-diastole for exercise induced stress at a heart rate of 150 bpm showing (**a**) raw aliased image, (**b**) image after spatial filter (SENSE), (**c**) image after temporal filter (UNFOLD), (**d**) image after combined adaptive spatiotemporal filter (TSENSE).

coils, increasing the demand for artifact suppression. Figures 3b and 4b are reconstructed using SENSE with adaptive coil estimates and Figs. 3c and 4c are reconstructed using temporal filtering (UNFOLD). Figures 3d and 4d are reconstructed using both spatial and temporal filtering using the adaptive TSENSE method. Both spatial and temporal filtering (applied separately) achieve a high degree of alias artifact suppression. Nevertheless, slight residual artifacts of the chest wall are apparent at these particular cardiac time phases. The chest wall artifact has been effectively removed using the adaptive TSENSE method with combined spatial and temporal filtering.

The suppression of alias artifacts can be estimated based on the temporal spectra of pixels, which contain a mixture of desired and aliased signal components. The average temporal spectrum of a small region containing the myocardium and aliased chest wall is shown in Fig. 5, with the region of interest indicated in the inset image. The power spectrum is calculated over approximately a 2-sec period using a hamming window and averaged over several dozen pixels. Figure 5a (solid bold line) is the spectrum of the raw unfiltered pixels with combined aliased and desired components. Figure 5b,c corresponds to the cases of SENSE and UNFOLD, respectively, when applied separately, and Fig. 5d (dashed bold line) is for adaptive TSENSE. Figure 5e is the magnitude frequency response of the UNFOLD temporal filter overlaid for reference. Note that the complex signal spectrum is highly asymmetric due to phase modulation resulting from tissue motion and blood flow.

Consider the temporal spectrum of the raw signal shown in Fig. 5a corresponding to a region in the central FOV (myocardium) with aliased peripheral FOV (back and chest). This spectrum is a mixture of aliased artifact and

myocardium signal. However, since the sample rate (31.2 Hz) is much greater than the modulation frequency (2.5 Hz) and since the envelope of the modulation spectrum for each signal falls off monotonically with increasing frequency, the mixture of artifact (back and chest) and true (myocardium) signals is dominated by the myocardium signal at the band center and by the artifact at the band edge. In other words, the value of the raw spectrum mixture in Fig. 5a is assumed to be all artifact at the band edge (±15.6 Hz in this example) and all true signal at band center (0 Hz). The error in this assumption is quite small since the true signal (and artifact) are down by approximately 30 dB or more at the band edges, as verified by normal imaging at slower rates (15–20 images per second). With the parameters used in this example, this assumption is fairly good even for modulation components at ±13.1 and ±10.6 Hz, corresponding to the first and second harmonics of the heart rate (2.5 Hz), respectively. Under this assumption, we will estimate and compare the artifact suppression for each method at the band edge, as well as at first and second harmonic modulation frequencies.

The chest wall component shifted to the band edge is very strong due to the proximity to the surface coil. The UNFOLD temporal filter easily suppresses the average component of the chest wall signal (band edge component) by at least 50 dB. Chest wall motion causes the temporal spectrum to have components at both the breathing rate and the heart rate. The heart rate modulation, although approximately 25 dB below the average chest wall intensity, is roughly only 15 dB below the myocardium signal of interest and is detectable if not further suppressed. In this example with exercise stress, the heart rate modulation is at 2.5 Hz (150 bpm); therefore, harmonics of the heart rate induced chest wall modulation are evident within the transition band (at ±13.1 Hz) and passband (at ±10.6 Hz) of the temporal low-pass filter. The UNFOLD low-pass cut-off would have to be reduced significantly in order to completely suppress these components, thereby removing
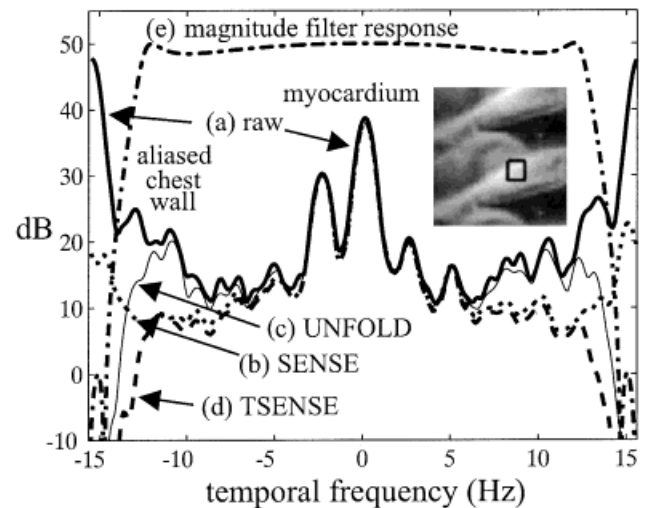
FIG. 5. Average temporal spectrum of a region (indicated on inset image) with both heart and aliased chest wall components: (**a**) raw signal, (**b**) SENSE, (**c**) UNFOLD, (**d**) adaptive TSENSE, and (**e**) temporal low-pass filter response.

the advantage of this method for accelerated imaging. These artifacts are readily observed in the UNFOLD images of Figs. 3c and 4c.

Artifact suppression at these frequencies may be measured from Fig. 5 as follows. The first harmonic component of heart rate modulation (± 13.1 Hz) is ~22–25 dB below the average chest wall component (at ± 15.6 Hz) and ~12–15 dB below the average myocardium (0 Hz). This component falls just outside the cut-off of the temporal filter, which provides only about 10 dB rejection at this frequency, as seen in Fig. 5e. With only 10 dB artifact suppression, the artifact is still above the noise. The artifact component at ± 10.6 Hz falls within the temporal filter passband, and thus has no temporal filter suppression. At this modulation frequency the artifact is 25–28 dB below the value at the band edge (± 15.6 Hz) but is less than 20 dB below the myocardium signal and estimated to be greater than 10 dB above the noise.

It is more difficult to realize adequate suppression (50 dB) of the intense chest wall over the full respiratory cycle using strictly spatial filtering. The average artifact using SENSE (slow adaptive) is suppressed approximately 30 dB by comparing Fig. 5a and b at the band edges, removing most of the static component. A small peak at ± 15.1 Hz due to the 0.5 Hz respiratory rate (30 breaths per minute) is evident in this example. The artifact corresponding to this residual component is seen in the SENSE images shown in Figs. 3b and 4b, particularly in the vicinity of posterior-lateral wall of myocardium and lung area. Fortunately, this respiratory component may be easily suppressed with temporal filtering. The UNFOLD temporal filter has a minimum stopband rejection of 50 dB (stop band for this filter is approximately 15–15.6 Hz). Thus, the average artifact for either UNFOLD or TSENSE (at 15.6 Hz) is well below the noise as seen in Fig. 5c,d. Adaptive SENSE or TSENSE suppresses the modulation components at ± 13.1 Hz and ± 10.6 Hz to near the apparent noise floor, with observed suppression of at least 15 dB, and more probably close to the 30 dB measured at the band edge.

The estimated values for artifact suppression for each method are summarized in Table 1 for the three temporal frequency components discussed above. From this table and preceding discussion, it can be seen that the TSENSE method achieves increased suppression over either SENSE or UNFOLD applied individually. The ratio of average myocardium signal to worst-case artifact component increased from approximately 20 dB using either SENSE or UNFOLD to greater than 30 dB using TSENSE. Thus, the static components at the band edge, which are strongest,

FIG. 6. Average temporal spectrum of a region (indicated on inset image) with both desired and aliased heart components: (**a**) raw signal, (**b**) SENSE, (**c**) UNFOLD, (**d**) adaptive TSENSE, and (**e**) temporal low-pass filter response.

are easily filtered temporally with excellent suppression and weaker components within the desired temporal passband are readily spatially filtered. TSENSE takes advantage of this complementary behavior. Another benefit of the TSENSE method is the inherent ability to quantitatively analyze artifact suppression using the temporal spectrum for those temporal frequencies for which the artifact and desired components may be distinguished.

It is further observed that the TSENSE method, unlike UNFOLD, may image the full FOV with a wide temporal bandwidth despite the fact that the central portion of the FOV is dynamic. This is demonstrated in Fig. 6, which shows the average temporal spectrum of an ROI in the outer FOV where the heart is aliased onto the outer FOV (reverse situation from Fig. 5). In this case, the relatively static outer FOV corresponds to the central component with narrow bandwidth, while the heart spectra (shifted to the band edge) occupies most of the temporal bandwidth. The average artifact suppression of the aliased heart component for this ROI is greater than 40 dB using SENSE as observed by comparing Fig. 6a and b at the band edge, and appears to be suppressed at or below the noise level across the full spectrum. The UNFOLD method by itself achieves excellent suppression at the band edge, but within the passband (-12.5 to $+12.5$ Hz) the peak artifact level is less than 10 dB below the desired component and between 10–20 dB above the estimated noise, since the temporal filter provides no suppression within the passband. This artifact from the heart into the outer portion of FOV is evident in the temporally filtered reconstructed image shown in Fig. 4c, which used a fixed 80% fractional bandwidth over the full FOV.

In a study with 10 normal volunteers, it has been previously shown that accelerated imaging using UNFOLD at 31.2 frames per second can be used to image cardiac function during exercise induced stress (8). In this study, accelerated imaging consistently improved quantitative analysis of function. Using these same data, we have demonstrated that TSENSE further improves artifact suppression as compared to either UNFOLD or SENSE.

Table 1
Estimates of Artifact Suppression for Cardiac Exercise Stress Example Corresponding to Temporal Spectra Shown in Fig. 5

Method	Average artifact suppression at band edge (± 15.6 Hz)	First harmonic heart rate modulation component (± 13.1 Hz)	Second harmonic heart rate modulation component (± 10.6 Hz)
UNFOLD	>50 dB	~10 dB	~0 dB
SENSE	~30	≫15	≫15
TSENSE	>50	≫25	≫15

The formula for SNR (Eq. [4]) was validated by comparing SNR estimates from a series of 256 phantom images, reconstructed using full k-space data, as well as reconstructed using UNFOLD, SENSE, and TSENSE. The temporal low-pass filter had a noise bandwidth of 0.71 f_s calculated by numerical integration; therefore, the UNFOLD SNR loss factor is 1.2 in this case. The measured UNFOLD SNR loss factor, calculated by ratio of SNR estimates for full k-space images to UNFOLD images, was within 1% of predicted. Similarly, the same loss factor was measured comparing the SNR of SENSE and TSENSE images. The SENSE SNR loss factor was estimated (for each pixel) by comparing the SNR for full k-space images and SENSE images. Based on the SENSE SNR loss, the estimate for G_{SENSE} ranged from 1.1 to 1.3, which was within several percent of that calculated independently from the smoothed coil sensitivity profiles. Finally, the measured SNR loss for TSENSE relative to full k-space reconstruction agreed with Eq. [4] using the above loss factors, within a few percent.

The SNR loss may be reduced to some extent by regularization of the inverse solution, thereby trading off artifact suppression (4). The method of diagonal loading may be used as done in the context of adaptive antenna arrays (9,10) with ill-conditioned covariance matrix estimates. Reduced artifact suppression for the spatial filter (SENSE) may be acceptable in cases where overall combined spatial and temporal filtering provide sufficient suppression.

CONCLUSION

An adaptive spatial-temporal filter for accelerated MR imaging was developed and demonstrated. This method, based on combining sensitivity encoding with multicoil arrays (SENSE) and sequential interleaved k-space acquisition and temporal low-pass filtering (UNFOLD), produces an accelerated imaging method, referred to as TSENSE, which may be used with either real-time or retrospective cine imaging. Benefits of the adaptive scheme include the ability to tolerate body motion or a change in scan plane without reacquiring additional reference images. It may be used to reconstruct the full FOV with large temporal bandwidth. The TSENSE method has the potential to permit a more flexible trade-off of SENSE artifact rejection for SNR by adjustable regularization of the inverse solution in regions with ill-conditioned inverse solution.

A number of practical advantages accrue from incorporating temporal filtering with spatial sensitivity encoding (TSENSE). First, to achieve a given level of artifact suppression, each method individually has performance limitations and constraints. The stringent requirements for each method are somewhat relaxed when implemented in a combined manner. For example, the temporal low-pass filter transition bandwidth may be slightly wider, thus yielding a smoother time response, which is a benefit to quantitative analysis of time–intensity curves. The coil sensitivity estimates can tolerate some additional errors since the static portion of the alias artifact is suppressed by means of temporal low-pass filtering. The TSENSE method facilitates quantitative measurement of artifact suppression by analysis of the temporal spectra.

The TSENSE method was demonstrated with nonbreath-held cardiac imaging during exercise stress with heavy breathing. In this case, the assumption that the coil sensitivities is static is not completely valid and artifacts were evident using SENSE with a four-element cardiac surface coil and $R = 2$ acceleration. A specific coil design employing a six-element design optimized for cardiac imaging (11) was utilized for imaging during stress, resulting in good quality images with only slight effects on image quality due to stress reported (12). In our study, the TSENSE method provided additional suppression (over using SENSE) at minimal cost in temporal bandwidth.

A drawback of the adaptive method for coil sensitivity estimation is that the k-space acquisition is optimized for speed rather than best image quality. Therefore, alias image suppression may be degraded by imaging artifacts such as echo planar imaging (EPI) ghosts and wrap artifacts. However, the nonadaptive form of TSENSE, implemented with separate reference acquisition, accrues many of the benefits, including better artifact suppression with simpler design, increased tolerance to motion, and slightly improved SNR by trading off spatial filtering rejection by means of regularization.

TSENSE may also be used in conjunction with partial-Fourier acquisition (partial-echo or partial NEX) for increased imaging speed and/or variable density k-space sampling to obtain further artifact suppression by sampling central portion of k-space more frequently. The use of combined temporal filtering with spatial filtering is also fully applicable to SMASH (3).

ACKNOWLEDGMENTS

REFERENCES

1. Madore B, Glover GH, Pelc NJ. Unaliasing by Fourier encoding the overlaps using the temporal dimension (UNFOLD), applied to cardiac imaging and fMRI. Magn Reson Med 1999;42:813–828.
2. Pruessmann KP, Weiger M, Scheidegger MB, Boesiger P. SENSE: sensitivity encoding for fast MRI. Magn Reson Med 1999;42:952–962.
3. Sodickson DK, Manning W. Simultaneous acquisition of spatial harmonics (SMASH): fast imaging with radiofrequency coil arrays. Magn Reson Med 1997;38:591–603.
4. Sodickson DK. Tailored SMASH image reconstructions for robust in vivo parallel MR imaging. Magn Reson Med 2000;44:243–251.
5. Heidemann R, Griswold MA, Haase A, Jakob PM. Variable density AUTO-SMASH imaging. In: Proc 8th Scientific Meeting ISMRM, Denver, 2000. p 274.
6. Kellman P, McVeigh ER, Method for combining UNFOLD with SENSE or SMASH. In: Proc 8th Scientific Meeting ISMRM, Denver, 2000. p 1507.
7. Epstein FH, Wolff, SD, Arai AE. Segmented k-space fast cardiac imaging using an echo-train readout. Magn Reson Med 1999;41:609–613.
8. London JF, Epstein FH, Kellman P, Wassmuth R, Arai AE. Exercise cardiac stress testing using real-time MRI. In: Proc of RSNA Scientific Assembly and Annual Meeting, Chicago, 2000. p 240.
9. Haykin S. Adaptive filter theory, 3rd ed. Englewood Cliffs, NJ: Prentice-Hall; 1996.
10. Carlson BD. Covariance matrix estimation errors and diagonal loading in adaptive arrays. IEEE Trans Aerospace Electr Sys 1988;24:397–401.
11. Weiger M, Pruessmann KP, Gosele R, Leussler C, Roschmann P, Boesiger P. Specific coil design for SENSE: a six-element cardiac array. In: Proc of 7th Annual Meeting ISMRM, Philadelphia, 1999. 7:162.
12. Weiger M, Pruessmann KP, Boesiger P. Cardiac real-time imaging using SENSE. Magn Reson Med 2000;43:177–184.